

1 **Efficacy of Parainfluenza Virus 5 (PIV5)-vectored Intranasal COVID-19 Vaccine as**  
2 **a Single Dose Vaccine and as a Booster against SARS-CoV-2 Variants**

3

4 Ashley C. Beavis<sup>1,2</sup>, Zhuo Li<sup>1</sup>, Kelsey Briggs<sup>2</sup>, María Cristina Huertas-Díaz<sup>1,2</sup>, Elizabeth  
5 R. Wrobel<sup>2</sup>, Maria Najera<sup>1</sup>, Dong An<sup>2</sup>, Nichole Orr-Burks<sup>2</sup>, Jackelyn Murray<sup>2</sup>, Preetish  
6 Patil<sup>1</sup>, Jiachen Huang<sup>2</sup>, Jarrod Mousa<sup>2</sup>, Linhui Hao<sup>3</sup>, Tien-Ying Hsiang<sup>3</sup>, Michael Gale,  
7 Jr.<sup>3</sup>, Stephen B. Harvey<sup>4</sup>, S. Mark Tompkins<sup>2</sup>, Robert Jeffrey Hogan<sup>2</sup>, Eric R.  
8 Lafontaine<sup>2</sup>, Hong Jin<sup>1</sup> and Biao He<sup>1,2,#</sup>.

9

10 <sup>1</sup>CyanVac LLC, Athens, Georgia, 30602.

11 <sup>2</sup>Department of Infectious Diseases, College of Veterinary Medicine, University of  
12 Georgia, Athens, Georgia.

13 <sup>3</sup>Department of Immunology, Center for Innate Immunity and Immune Disease,  
14 University of Washington, Seattle, Washington.

15 <sup>4</sup>Animal Resources, University of Georgia, Athens, Georgia; Department of Population  
16 Health, College of Veterinary Medicine, University of Georgia, Athens, Georgia.

17 # Corresponding author: [bh1@cyanvacllc.com](mailto:bh1@cyanvacllc.com)

18

19

20  
21  
22  
23  
24  
25  
26  
27  
28  
29  
30  
31  
32  
33  
34  
35  
36  
37  
38  
39  
40

## Abstract

Immunization with severe acute respiratory syndrome coronavirus 2 (SARS-CoV-2) vaccines has greatly reduced coronavirus disease 2019 (COVID-19)-related deaths and hospitalizations, but waning immunity and the emergence of variants capable of immune escape indicate the need for novel SARS-CoV-2 vaccines. An intranasal parainfluenza virus 5 (PIV5)-vectored COVID-19 vaccine CVXGA1 has been proven efficacious in animal models and blocks contact transmission of SARS-CoV-2 in ferrets. CVXGA1 vaccine is currently in human clinical trials in the United States. This work investigates the immunogenicity and efficacy of CVXGA1 and other PIV5-vectored vaccines expressing additional antigen SARS-CoV-2 nucleoprotein (N) or SARS-CoV-2 variant spike (S) proteins of beta, delta, gamma, and omicron variants against homologous and heterologous challenges in hamsters. A single intranasal dose of CVXGA1 induces neutralizing antibodies against SARS-CoV-2 WA1 (ancestral), delta variant, and omicron variant and protects against both homologous and heterologous virus challenges. Compared to mRNA COVID-19 vaccine, neutralizing antibody titers induced by CVXGA1 were well-maintained over time. When administered as a boost following two doses of a mRNA COVID-19 vaccine, PIV5-vectored vaccines expressing the S protein from WA1 (CVXGA1), delta, or omicron variants generate higher levels of cross-reactive neutralizing antibodies compared to three doses of a mRNA vaccine. In addition to the S protein, the N protein provides added protection as assessed by the highest body weight gain post-challenge infection. Our data indicates that PIV5-

41 vectored COVID-19 vaccines, such as CVXGA1, can serve as booster vaccines against  
42 emerging variants.

43

#### 44 **Importance**

45 With emerging new variants of concern (VOC), SARS-CoV 2 continues to be a  
46 major threat to human health. Approved COVID-19 vaccines have been less effective  
47 against these emerging VOCs. This work demonstrates the protective efficacy, and  
48 strong boosting effect, of a new intranasal viral-vectored vaccine against SARS-CoV-2  
49 variants in hamsters.

50

51

52  
53  
54  
55  
56  
57  
58  
59  
60  
61  
62  
63  
64  
65  
66  
67  
68  
69  
70  
71  
72  
73

## Introduction

Severe acute respiratory syndrome coronavirus 2 (SARS-CoV-2) first emerged in Wuhan, China in December 2019 [1]. Since then, it has spread globally, infected more than 519 million people, and caused at least 6 million deaths (<https://covid19.who.int>). SARS-CoV-2 initially infects the upper respiratory tract epithelium [2] but can progress to the lower respiratory tract and cause pneumonia and acute respiratory distress syndrome (ARDS) [3]. Since the beginning of the 2019 coronavirus disease (COVID-19) pandemic, numerous SARS-CoV-2 variants have emerged. The World Health Organization (WHO) defines a SARS-CoV-2 variant of concern (VOC) as a variant that affects virus transmissibility and COVID-19 epidemiology, increases virulence and pathogenicity, or decreases the effectiveness of COVID-19 vaccines (immune escape). Current VOCs include delta and omicron, while previously circulating VOCs include alpha, beta, and gamma (<https://www.who.int/activities/tracking-SARS-CoV-2-variants>). The global spread of SARS-CoV-2 prompted rapid development of prophylactic vaccines. Currently, three vaccines are approved for use in the United States. The vaccines developed by Pfizer and Moderna are based on mRNA technology, while the vaccine produced by Johnson & Johnson (J&J) utilizes a human adenovirus type 26 vector. A vaccine produced by AstraZeneca employs a Chimpanzee adenovirus vector and is approved for use in the European Union and other countries [4]. Since May 2022, 11 billion vaccine doses have been administered worldwide (<https://covid19.who.int>). However, SARS-CoV-2 variants have demonstrated immune escape in previously

74 infected and fully vaccinated individuals. Compared to neutralization of alpha variant,  
75 serum from convalescent individuals was four-fold less effective against delta variant  
76 [5]. Similarly, serum from individuals who received two doses of Pfizer's vaccine has  
77 neutralizing antibody titers against delta variant three- to five-fold lower than alpha  
78 variant. This immune escape was correlated to amino acid changes in the antigenic  
79 epitopes of the SARS-CoV-2 spike protein [5]. A study found that the omicron-  
80 neutralizing ability of serum from WA1-convalescent individuals was eight-fold lower  
81 than its WA1-neutralizing ability [6]. For individuals vaccinated with Pfizer, Moderna,  
82 J&J, or AstraZeneca vaccines, vaccine efficacy decreased by approximately 21  
83 percentage points within one to six months after full vaccination, which was associated  
84 with waning immunity [7]. Due to waning immunity and the emergence of variants  
85 capable of immune escape, there is an urgent need for novel SARS-CoV-2 vaccine  
86 candidates with long-lasting protective immunity against the variants.

87         Parainfluenza virus 5 (PIV5) is a negative-sense, single-stranded, RNA virus in  
88 the family *Paramyxoviridae*. Its 15,246-nucleotide genome encodes for 8 proteins [8, 9].  
89 Previously, recombinant PIV5 viruses expressing foreign genes from numerous  
90 pathogens, including influenza, rabies, respiratory syncytial virus, *Tuberculosis*,  
91 *Burkholderia*, and MERS-CoV have been generated and tested as vaccine candidates  
92 preclinically [10-15]. Because it actively replicates in the respiratory tract following  
93 intranasal immunization, PIV5-vectored vaccines can generate mucosal immunity that  
94 includes antigen-specific IgA antibodies and long-lived IgA plasma cells [12, 16].  
95 Recently a PIV5-vectored vaccine expressing the spike protein from SARS-CoV-2

96 Wuhan (ancestral strain) (WA1; CVXGA1) has been shown to be efficacious in mice  
97 and ferrets [17]. A single, intranasal dose of CVXGA1 induced WA1-neutralizing  
98 antibodies and protected K18-hACE2 mice against lethal infection with SARS-CoV-2  
99 WA1. Furthermore, a single, intranasal dose of CVXGA1 protected ferrets from SARS-  
100 CoV-2 WA1 infection and blocked contact transmission to cohoused naïve ferrets [17].  
101 While these studies demonstrated its efficacy against SARS-CoV-2 WA1, CVXGA1's  
102 efficacy against SARS-CoV-2 variants was not tested.

103         Golden Syrian hamsters have been proven susceptible to infection with SARS-  
104 CoV-2. Chan, et al. showed that following infection with WA1, hamsters lost weight for 6  
105 days before starting to recover [18]. SARS-CoV-2 vRNA was detected in nasal  
106 turbinate, trachea, and lungs of infected hamsters, and peak infectious viral titer in the  
107 nasal turbinate and lungs was measured at 4 days post-infection [18]. While these  
108 studies used WA1 strain, several studies have since shown that hamsters are  
109 susceptible to infection with alpha and delta variants [19-21]. Among VOC alpha, delta,  
110 and omicron, delta causes the most weight loss and has the best viral replication in  
111 lungs of infected hamsters; omicron VOC, even with a high dose infection ( $2.5 \times 10^6$  PFU  
112 per animal) did not cause weight loss, and replicates poorly in the lower respiratory tract  
113 of infected hamsters [22].

114         CVXGA1, recombinant PIV5 expressing S from SARS-CoV-2 WA1, is currently  
115 under phase 1 clinical trial in the US [23]. In this work, we examined efficacy of  
116 CVXGA1, and other recombinant PIV5 vaccines expressing S from SARS-CoV-2 beta,  
117 gamma, delta, or omicron, as a single-dose intranasal vaccine and as a boost following

118 vaccination with two doses of COVID-19 mRNA vaccine against challenge infection with  
119 WA1, alpha, and delta in a Golden Syrian hamster model.

120

121

122

## Materials and Methods

### 123 Cells

124 Vero E6 cells were maintained in Dulbecco's modified Eagle media (DMEM)  
125 supplemented with 5% fetal bovine serum (FBS) plus 100 IU/mL penicillin and  
126 100ug/mL streptomycin (1% P/S; Mediatech Inc, Manassas, VA, USA). Serum-free (SF)  
127 Vero cells were maintained in VP-SFM (ThermoFisher Scientific) plus 4mM GlutaMax  
128 (Gibco). Vero-TEMPRSS cells were obtained from Dr. Jeff Hogan, University of  
129 Georgia, and maintained in DMEM + 10% FBS + 1mg/mL G418. All cells were  
130 incubated at 37°C, 5% CO<sub>2</sub>.

131

### 132 Plasmids and virus rescue

133 The construction of a plasmid encoding for PIV5 antigenome and generation of  
134 recombinant PIV5 were as previously described [24]. To construct plasmids encoding  
135 the antigenome of CVXGA1, CVXGA3, CVXGA5, CVXGA13, and CVXGA14, the Spike  
136 (S) genes from SARS-CoV-2 WA1, alpha, gamma, delta, and omicron, respectively,  
137 were placed as an additional open reading frame (ORF) transcription unit between the  
138 PIV5 SH and HN genes. The S cytoplasmic tail was replaced by the PIV5 fusion (F)  
139 protein cytoplasmic tail. To construct CVXGA2, encoding both the SARS-CoV-2 WA1  
140 nucleoprotein (N) and S proteins, the N gene was placed as an additional ORF  
141 transcription unit between the PIV5 HN and L genes of CVXGA1. Primer sequences are  
142 available upon request. To generate recombinant PIV5 viruses CVXGA1, CVXGA2,  
143 CVXGA3, CVXGA5, CVXGA13, and CVXGA14, plasmids encoding the PIV5

144 antigenomic cDNA, the supporting plasmids (PIV5-NP, P, L), and T7 polymerase were  
145 transfected into serum-free (SF) Vero cells by FuGene transfection reagent (Fugent) or  
146 electroporation (Neon transfection system, Invitrogen). Recovered virus was amplified in  
147 SF Vero cells and the viral genomes were verified by RT-PCR and Sanger sequencing.

148

## 149 **Virus propagation**

150         The recombinant PIV5 viruses were propagated in SF Vero cells at a multiplicity  
151 of infection (MOI) 0.001 PFU in VP-SFM + 4mM GlutaMax for 5 to 7 days at 37°C with  
152 5% CO<sub>2</sub>. The media was collected and centrifuged at 1,500 rpm for 10 mins to pellet  
153 cell debris. The supernatant was mixed with 0.1 volume of 10X sucrose-phosphate-  
154 glutamate (SPG) buffer or 10X SPG + 10% Arginine, aliquoted, flash-frozen in liquid  
155 nitrogen, and stored at -80°C. The PIV5 virus stocks were titrated by plaque assay in  
156 Vero cells followed by immunostaining.

157         The SARS-CoV-2 viruses were propagated in Vero cells with DMEM + 1% FBS +  
158 1X P/S. WA1 (BEI NR-52281) and alpha variant (USA/CA\_CDC\_5574/2020; BEI NR-  
159 54011) were obtained from BEI Resources. The omicron variant was provided by Dr.  
160 Jeff Hogan, University of Georgia. The delta variant was provided by Dr. Michael Gale,  
161 Jr., University of Washington. For isolation and production of delta variant stock, SARS-  
162 CoV-2 positive specimens with Ct < 33 were identified from reference testing [25]. The  
163 positive specimens were transferred to a biosafety level (BSL) 3 laboratory for virus  
164 culture. The virus transport medium (VTM) was first cleaned by filtering through Corning  
165 Costar Spin-X centrifuge tube filter (CLS8160), 0.1 mL of the cleaned VTM was used to

166 infect Vero E6 cells ectopically expressing human ACE2 and TMPRSS2 (VeroE6-AT  
167 cells; a gift from Dr. Barney Graham, National Institutes of Health, Bethesda MD) in a  
168 48-well plate. Two to four days post-infection when cytopathic effect, typical of SARS-  
169 CoV-2 infection, was observed, culture supernatants were collected and designated as  
170 a passage P0 virus stock. P1 virus stock cultures were grown in Vero E6/TMPRSS2  
171 cells (JCRB1819) using P0 virus as inoculum. The titer of the P1 stock was measured  
172 by standard SARS-CoV-2 plaque assay as described [26].

173 P1 stock virus was verified with whole genome sequencing analysis. An aliquot  
174 of P1 stock was subject to RNA extraction (Zymo Research, R1040) and used as  
175 template to produce cDNA with SuperScript™ IV First-Strand Synthesis System  
176 (ThermoFisher, Waltham, MA, USA). The products were then subject to library  
177 production using the Swift SARS-CoV148 2 SNAP Version 2.0 kit (Swift Biosciences™,  
178 Ann Arbor, MI, USA) following the manufacturer's instructions. Resulting libraries were  
179 quality-assessed using the Agilent 4200 TapeStation (Agilent Technologies, Santa Clara,  
180 CA, USA). Libraries with concentrations of 1.0 ng/μL were then sequenced on an  
181 Illumina NextSeq 500 (Illumina, San Diego, CA, USA) along with positive and negative  
182 controls.

183 The sequence data was processed through covid-swift-pipeline  
184 ([https://github.com/greninger-lab/covid\\_swift\\_pipeline](https://github.com/greninger-lab/covid_swift_pipeline)). Consensus genome sequences  
185 were generated by aligning the amplicon reads to the SARS-CoV-2 Wuhan-Hu-1  
186 ancestral reference genome (NC\_045512.2). For each genome, at least 1 million raw  
187 reads were acquired, representing >750x mean genome coverage and a minimum of

188 10x base coverage. Each consensus genome was then analyzed using the  
189 Phylogenetic Assignment of Named Global Outbreak Lineages (pangolin) tool to assign  
190 lineage based on the Pangolin dynamic lineage nomenclature scheme [27], defining the  
191 delta variant stock as Pangolin B.1.617.2.

192

### 193 **Immunofluorescence assay (IFA)**

194 Immunofluorescence assays were performed to examine protein expression in  
195 virus-infected Vero cells. Vero cells were infected at MOI 0.01 with PIV5, CVXGA1,  
196 CVXGA2, CVXGA3, CVXGA5, CVXGA13, or CVXGA14 for 3 days before being fixed  
197 with 80% methanol. The cells were incubated with mouse anti-PIV5 V/P monoclonal  
198 antibody (PK 366), rabbit anti-SARS-CoV-2 S (Sino Biological catalog no. 40150-R007),  
199 or SARS-CoV-2 N (ProSci catalog no. 35-579) antibodies at 1:500 in PBS + 3% bovine  
200 serum albumin (BSA) for 1 hr. Next, the cells were washed with PBS and incubated with  
201 goat  $\alpha$ -mouse Cy3 (KPL) or goat  $\alpha$ -rabbit Cy3 (KPL) at 1:500 in PBS + 3% BSA for 30  
202 mins. The cells were washed with PBS and imaged with an EVOS M5000 microscope  
203 (Thermo Fisher Scientific).

204

### 205 **Hamsters**

206 Five-to-seven-week-old Golden Syrian hamsters were obtained from Charles  
207 River Laboratories. The hamsters were single housed in animal BSL2 (ABSL2) facilities  
208 with ad libitum access to food and water. Pre-challenge procedures were performed at  
209 the University of Georgia Biological Sciences Animal Facility. The hamsters were

210 transferred to BSL3 facilities in the University of Georgia Animal Health Research  
211 Center (ABSL3) for the challenge and post-challenge procedures. The hamsters were  
212 anesthetized for immunization, blood collection, and challenge by intraperitoneal  
213 injection of 100  $\mu$ L ketamine/acepromazine cocktail. All experiments were performed in  
214 accordance with protocols approved by the Institutional Animal Care and Use  
215 Committee at the University of Georgia.

216

### 217 **Immunization and challenge of hamsters**

218 To administer intranasal immunizations, anesthetized hamsters were placed on  
219 their backs, a pipette was used to dispense 100  $\mu$ L inoculum onto their noses, and the  
220 inoculum was allowed to drain into their respiratory tracts. They were recovered on  
221 heating pads.

222 A COVID-19 mRNA vaccine was obtained from a clinical site, reconstituted to  
223 200  $\mu$ g/mL, aliquoted, and stored at  $-80^{\circ}\text{C}$ . Two  $\mu$ g mRNA vaccine in 50  $\mu$ L was  
224 administered via intramuscular injection.

225 For study AE19 (Figure 4), hamsters (n=8) received a single intranasal  
226 immunization of 100  $\mu$ L of  $10^5$  plaque-forming units (PFU) PIV5, CVXGA1, CVXGA2,  
227 CVXGA3, or CVXGA5. At 28 days post-immunization (dpi), blood was collected from  
228 the hamster saphenous vein for serological analysis. At 36 dpi, the hamsters were  
229 anesthetized: four hamsters were challenged intranasally with 30  $\mu$ L  $10^3$  PFU of SARS-  
230 CoV-2 Wuhan strain (WA1), and the remaining four hamsters were challenged with  $10^3$   
231 PFU SARS-CoV-2 alpha variant (CA; BEI NR54011) as previously reported by

232 Blanchard, et al. [28]. Following challenge infection, the hamster weights were  
233 monitored for 5 days. At 5 days post-challenge (dpc), the hamsters were euthanized,  
234 and the hamster lungs were harvested, resuspended in 2 mL DMEM + 2% FBS + 1X  
235 antibiotic/antimycotic, homogenized, aliquoted, and stored at -80°C. SARS-CoV-2 viral  
236 burden in lung homogenate was quantified via plaque assay and real-time quantitative  
237 reverse transcription polymerase chain reaction (RT-qPCR).

238 For study AE23 (Figure 5), hamsters received intramuscular (i.m.) immunizations  
239 of 100  $\mu$ L PBS (n=20, group 1) or 2  $\mu$ g mRNA COVID-19 vaccine (n=20, group 2). At 21  
240 dpi, hamsters that received the mRNA vaccine were boosted with the mRNA vaccine. At  
241 28 dpi, blood was collected from the hamster saphenous vein for serological analysis.  
242 At 35 dpi following initial immunization, hamsters that received PBS during the first  
243 immunization received either 100  $\mu$ L of PBS intranasally (i.n.) (n=5, group 1A),  $3 \times 10^5$   
244 PFU CVXGA1 (n=5, group 1B),  $2 \times 10^5$  PFU CVXGA3 (n=5, group 1C), or  $1.5 \times 10^5$  PFU  
245 CVXGA13 (n=5, group 1D). Group 2 hamsters that received two doses of mRNA  
246 received 100  $\mu$ L of PBS (n=4, group 2A),  $3 \times 10^5$  PFU CVXGA1 (n=4, group 2B),  $2 \times 10^5$   
247 PFU CVXGA3 (n=4, group 2C),  $1.5 \times 10^5$  PFU CVXGA13 (n=4, group 2D) i.n., or a third  
248 dose of mRNA i.m. (n=4, group 2E). Hamsters were anesthetized for intranasal  
249 immunizations but not intramuscular injections. Blood was collected at 54 dpi. At 63 dpi,  
250 the hamsters were challenged with  $10^4$  PFU SARS-CoV-2 delta variant. Following  
251 challenge infection, hamster weights were monitored for 5 days. At 5 dpc, the hamsters  
252 were euthanized, their lungs were harvested, and the SARS-CoV-2 viral burden was  
253 quantified via plaque assay and RT-qPCR.

254 For study AE24 (Figures 6 and 7), hamsters received 100  $\mu$ L of PBS i.n. (n=5,  
255 Group 1), 2  $\mu$ g mRNA COVID-19 vaccine i.m. (n=25, Group 2), or 100  $\mu$ L  $7 \times 10^4$  PFU  
256 CVXGA1 i.n. (n=10, Groups 3 & 4). At 29 dpi, the hamsters that received the mRNA  
257 vaccine were boosted with the mRNA vaccine i.m. and the group 3 hamsters received  
258 another dose of CVXGA1 i.n. At 91 dpi following initial immunization, hamsters who  
259 received two doses of mRNA received either 2  $\mu$ g mRNA vaccine i.m. (n=5, Group 2A)  
260 or 100  $\mu$ L of  $7 \times 10^4$  PFU CVXGA1 (n=5, Group 2B),  $10^3$  PFU CVXGA13 (n=5, Group  
261 2C), PBS i.n. (n=5, Group 2D), or  $10^4$  PFU CVXGA14 (n=5, Group 2E). Hamsters were  
262 anesthetized for intranasal immunizations but not intramuscular injections. At 36 and  
263 108 dpi, blood was collected via the hamster gingival vein. At 116 dpi, the hamsters  
264 were challenged with 30  $\mu$ L of  $10^4$  PFU SARS-CoV-2 delta variant. Following challenge  
265 infection, hamster weights were monitored for 5 days. The hamster lungs were  
266 harvested, and SARS-CoV-2 viral burden was quantified via plaque assay and RT-  
267 qPCR.

268 All animal experiments were performed according to the protocols approved by  
269 the Institutional Animal Care and Use Committee at the University of Georgia.

270

### 271 **Enzyme-linked immunosorbent assay (ELISA)**

272 To quantify the anti-SARS-CoV-2 S and RBD humoral response, hamster serum  
273 was analyzed via ELISA. Immulon® 2HB 96-well microtiter plates were coated with 100  
274  $\mu$ L SARS-CoV-2 S or RBD at 1  $\mu$ g/mL. For all ELISAs, plates were coated with SARS-  
275 CoV-2 S and RBD from the WA1 strain, which were produced and purified as described

276 previously [17]. Hamster serum was serially diluted two-fold and incubated on the plates  
277 for 2 hrs. Horseradish peroxidase-labelled goat anti-mouse IgG secondary antibody  
278 (Southern Biotech, Birmingham, Alabama) was diluted 1:2000 and incubated on the  
279 wells for 1 hr. The plates were developed with KPL SureBlue Reserve TMB Microwell  
280 Peroxidase Substrate (SeraCare Life Sciences, Inc., Milford, Massachusetts), and  
281 OD<sub>450</sub> values were obtained with a BioTek Epoch Microplate Spectrophotometer  
282 (BioTek, Winooski, Vermont). Antibody titers were calculated as log<sub>10</sub> of the highest  
283 serum dilution at which the OD<sub>450</sub> was greater than two standard deviations above the  
284 mean OD<sub>450</sub> of naïve serum.

285

## 286 **Neutralization assays**

287 To quantify the SARS-CoV-2-neutralizing antibodies generated by the hamsters,  
288 microneutralization assays were performed in a BSL 3 facility. Hamster serum was  
289 heat-inactivated at 56°C for 45 mins and serially diluted two-fold. The serum was mixed  
290 1:1 with 6x10<sup>3</sup> focus-forming units (FFU)/mL SARS-CoV-2 WA1, delta, or omicron  
291 variants. The serum/virus mixture was incubated at 37°C for 1 hr before being incubated  
292 on 96-wells of Vero cells for WA1 or Vero TEMPRSS2 cells for delta and omicron,  
293 respectively. One hour post-infection, a methylcellulose overlay (DMEM + 5% FBS +  
294 1% P/S + 1% methylcellulose) was added on top of the serum/virus mixture. The plates  
295 were incubated at 37°C, 5% CO<sub>2</sub> for 24 hrs. After removal of the methylcellulose  
296 overlay, the wells were washed with PBS, and the cells were fixed with 60%  
297 methanol/40% acetone, followed by immunostaining with anti-SARS-CoV-2 N antibody

298 (ProSci catalog no. 35-579). The number of infected cells were quantified via Cytation 7  
299 imaging reader (BioTek). Neutralization titers were calculated as log<sub>10</sub> of the highest  
300 serum dilution at which the virus infectivity was reduced by at least 50%.

301

### 302 **Plaque assay for infectious virus titer**

303 To quantify infectious SARS-CoV-2 in lung homogenates, plaque assays were  
304 performed. For the plaque assays, lung homogenates were serially diluted in DMEM +  
305 2% FBS + 1% antibiotic/antimycotic and added to 12-well plates of Vero E6 cells for  
306 SARS-CoV-2 WA1 and alpha variant or Vero TEMPRSS2 cells for delta and omicron  
307 variants. At 1 hour post-infection, the inoculum was removed, and a methylcellulose  
308 overlay (500mL Opti-MEM + 0.8% methylcellulose + 2% FBS + 1%  
309 antibiotic/antimycotic) was added to the wells. Following incubation for 3 days, the  
310 overlay was removed, and the cells were fixed with 60% methanol/40% acetone. After  
311 staining with crystal violet, the number of plaques were counted, with viral titers  
312 expressed as PFU/mL of lung homogenate.

313

### 314 **qPCR**

315 SARS-CoV-2 viral RNA levels were quantified by RT-qPCR. SARS-CoV-2 virus  
316 was inactivated by mixing 100 µL lung homogenate with 900 µL TRIzol (Invitrogen).  
317 Using a QIAgen RNA extraction kit, RNA was extracted from 140 µL  
318 homogenate/TRIzol and eluted in 15 µL of elution buffer, of which 5 µL was used in the  
319 qRT-PCR reaction. qRT-PCR was performed according to the protocol described in the

320 “CDC 2019-Novel Coronavirus (2019-nCoV) Real-Time RT-PCR Diagnostic  
321 Panel...Instructions for Use” (page 26; <https://www.fda.gov/media/134922/download>)  
322 with Applied Biosystems TaqPath One Step RT qPCR Master Mix and SARS-CoV-2  
323 Research Use Only qPCR Primer and Probe Kit primer/probe mix N1. SARS-CoV-2  
324 viral RNA was extracted from 140  $\mu$ L of SARS-CoV-2 WA1, alpha variant, and delta  
325 variant viruses of known titers and eluted in 15  $\mu$ L of elution buffer. The viral RNA was  
326 serially diluted 10-fold and 5  $\mu$ L from each dilution was used in the RT-qPCR assay. To  
327 generate a standard curve, the viral titer was plotted on the x-axis and the CT value was  
328 plotted on the y-axis. The standard curves were used to calculate the CT value that  
329 corresponds to 1 PFU/rxn in virus stock and hamster lung homogenates. The CT value  
330 of RNA extracted from sterile elution buffer was designated the PCR negative cutoff.

331

332

## Results

333

### 334 **Construction and characterization of PIV5-vectored SARS-CoV-2 vaccines**

335         We previously generated a PIV5-vectored vaccine for SARS-CoV-2 by inserting  
336 the SARS-CoV-2 WA1 S gene, which had the cytoplasmic tail of the S protein replaced  
337 with the cytoplasmic tail from the PIV5 F protein, between the PIV5 SH and HN genes  
338 (CVXGA1). We showed that a single, intranasal dose of CVXGA1 protects K18-hACE2  
339 mice from lethal infection with the WA1 strain, the initial circulating strain in the US, and  
340 blocks contact transmission in ferrets [17]. To determine whether expressing the N  
341 protein of SARS-CoV-2 as an additional antigen enhances protection afforded by the S  
342 antigen alone, we generated PIV5 expressing both S and N (CVXGA2). During our  
343 study period, SARS-CoV-2 VOCs emerged and some became dominant strains at  
344 different times. Thus, we generated PIV5-vectored vaccine candidates expressing S  
345 from SARS-CoV-2 VOC in a similar manner as CVXGA1 (Figure1): variants beta  
346 (CVXGA3), gamma (CVXGA5), delta (CVXGA13), and omicron (CVXGA14) (collectively  
347 called CVXGA vaccines). All variant S genes had the cytoplasmic tail replaced with the  
348 PIV5 F cytoplasmic tail.

349         The vaccine viruses were recovered as previously described, and their genomes  
350 were confirmed by RT-PCR and sequencing [29]. Compared to PIV5 vector-infected  
351 cells, all PIV5-vectored vaccines had increased syncytia, indicating that SARS-CoV-2 S  
352 is functional (Figure 2A).

353 To further confirm antigen expression, Vero cells were infected at MOI 0.01 with PIV5,  
354 CVXGA1, CVXGA2, CVXGA3, CVXGA5, CVXGA13, or CVXGA14 and assayed for  
355 immunofluorescence with WA1 S-specific antibody or N-specific antibody for CVXGA2.  
356 As expected, S expression was detected in cells infected with CVXGA1, 2, 3, 5, 13 and  
357 14. Additionally, SARS-CoV-2 N expression was detected in cells infected with  
358 CVXGA2 (Figure 2B).

359

### 360 **PIV5-vectored SARS-CoV-2 vaccines induce an anti-S humoral response in** 361 **hamsters**

362 To test efficacy of PIV5-vectored COVID-19 vaccine candidates in hamsters,  
363 their ability to induce S-specific antibody responses in hamsters was examined. We  
364 immunized Golden Syrian hamsters with a single, intranasal dose of  $10^5$  plaque-forming  
365 units (PFU) PIV5 vector, CVXGA1, CVXGA2, CVXGA3, or  $5 \times 10^2$  PFU CVXGA5 (Figure  
366 3A). While hamsters immunized with PIV5 vector had no detectable anti-SARS-CoV-2-S  
367 binding antibodies at day 28 dpi, a single intranasal dose of CVXGA1, CVXGA2, or  
368 CVXGA3 induced mean ELISA antibody titers of over 10,000. Even CVXGA5, at a lower  
369 immunization dose, was able to induce an anti-S ELISA titer greater than 9,333 (Figure  
370 3B).

371

### 372 **CVXGA vaccines protect against homologous and heterologous challenges**

373 To assess the efficacy of PIV5-vectored SARS-CoV-2 vaccines against  
374 homologous and heterologous virus challenges, CVXGA-immunized hamsters were

375 challenged with either  $10^3$  PFU SARS-CoV-2 WA1 (USA-WA01/2020) or alpha variant  
376 (CA; BEI NR54011) at 36 dpi. The hamster weights were monitored daily for 5 days  
377 post-challenge (dpc). Following challenge with WA1, hamsters immunized with PIV5  
378 vector lost weight and did not recover before the study was terminated. In contrast,  
379 hamsters immunized with CVXGA1, CVXGA2, CVXGA3, or CVXGA5 lost weight at day  
380 1 post-challenge but returned to pre-challenge weights 3 to 4 dpc (Figure 4A). While  
381 challenge with alpha variant induced less severe weight loss in PIV5 vector-immunized  
382 hamsters, hamsters immunized with CVXGA1, CVXGA2, CVXGA3, or CVXGA5 had  
383 significantly higher body weights compared to PIV5 vector-immunized hamsters at 5  
384 dpc. In both virus challenge groups, hamsters immunized with CVXGA2 had the highest  
385 mean body weight gains following challenge (Figure 4B), suggesting that the SARS-  
386 CoV-2 N antigen provided additional protection.

387 To quantify challenge viral burden in the lungs, infectious virus in lung  
388 homogenates was quantified by plaque assay. Hamsters immunized with PIV5 vector  
389 had infectious SARS-CoV-2 virus titer greater than  $4 \log_{10}$  PFU/mL lung homogenate  
390 following challenge with WA1 or alpha variant, while no infectious WA1 or alpha variant  
391 was detected in hamsters immunized with CVXGA1, CVXGA2, CVXGA3, or CVXGA5  
392 (Figures 4C & D; limit of detection, LOD, 25 PFU/mL). Viral RNA in the lung was  
393 quantified by RT-qPCR. Hamsters immunized with PIV5 vector and challenged with  
394 WA1 or alpha variant had mean cycle threshold (CT) values of 15.9 and 13.5,  
395 respectively (Figures 4E & F). Following challenge with WA1 or alpha variant, hamsters  
396 that received a single intranasal dose of CVXGA1 or CVXGA2 had CT values indicative

397 of less than 1 PFU per reaction (PFU/rxn). CVXGA3-immunized hamsters had CT  
398 values indicative of less than 1 PFU/rxn following challenge with WA1 but two hamsters  
399 had CT values equating to 1 or 96 PFU/rxn following challenge with alpha variant  
400 (Figures 4E & F, Supplemental figure 1). A single dose of CVXGA2 performed the best  
401 against heterologous challenge with alpha variant (Figure 4F), suggesting that SARS-  
402 CoV-2 N might offer additional protection.

403

#### 404 **CVXGA vaccines protect against delta challenge**

405 As of May 2022, delta variant is one of two VOCs circulating in the United States  
406 (<https://www.who.int/activities/tracking-SARS-CoV-2-variants>). Therefore, we assessed  
407 the efficacy of our lead vaccine candidate, CVXGA1, against heterologous challenge  
408 with delta variant and tested a vaccine expressing S from delta variant against  
409 homologous challenge. Hamsters received a single, intranasal dose of PBS or  $10^5$  PFU  
410 of CVXGA1, CVXGA3, or CVXGA13. At 19 dpi, blood was collected and serum anti-  
411 SARS-CoV-2 WA1 S and -RBD IgG antibodies were quantified via ELISA (Figure 5A).  
412 CVXGA1, CVXGA3, or CVXGA13 elicited anti-S antibodies with mean titers of over  
413 10,000 (Figure 5B). Interestingly, hamsters immunized with CVXGA13 had the highest  
414 level of anti-WA1 RBD antibodies with a mean titer of 50,119 (Figure 5C).

415 At 28 dpi, the hamsters were intranasally challenged with  $10^4$  PFU SARS-CoV-2  
416 delta variant and their weights were monitored for 5 days. Beginning at 2 dpc, hamsters  
417 immunized with PBS experienced weight loss that steadily declined until the study was  
418 terminated. In contrast, hamsters immunized with CVXGA1, CVXGA3, or CVXGA13

419 experienced weight gain after 2 dpc. While not statistically significant, hamsters  
420 immunized with CVXGA13 had greater weight gain than hamsters immunized with  
421 CVXGA1 or CVXGA3, indicating that PIV5 expressing S from SARS-CoV-2 delta variant  
422 protected hamsters the best from weight loss following homologous challenge with delta  
423 variant (Figure 5D). To further assess the vaccine efficacy, challenge virus load in lungs  
424 at 5 dpc were examined by plaque assay and RT-qPCR. While hamsters immunized  
425 with CVXGA1, CVXGA3, or CVXGA13 did not have detectable infectious challenge  
426 virus in their lung homogenates, hamsters immunized with PBS had a mean titer of  $3 \times$   
427  $10^4$  PFU/mL lung homogenate (Figure 5E). Four of five hamsters immunized with  
428 CVXGA1 and all hamsters immunized with CVXGA3 or CVXGA13 had CT values  
429 indicative of no infectious virus. One CVXGA1-immunized hamster had a CT value of  
430 26.39 (Figure 5F). The weight loss and lung viral burden data from this study  
431 demonstrated that single, intranasal doses of CVXGA1 and CVXGA3 protect hamsters  
432 from heterologous challenge and CVXGA13 protects hamsters from homologous  
433 challenge with delta variant. The protective effect offered by CVXGA13 against  
434 homologous delta virus is the best among the three CVXGA vaccine candidates.

435

### 436 **CVXGA1 generates longer lasting immunity**

437 As of May, 2022, 67 percent of individuals in the United States are fully  
438 vaccinated against COVID-19 ([https://ourworldindata.org/covid-](https://ourworldindata.org/covid-vaccinations?country=USA)  
439 [vaccinations?country=USA](https://ourworldindata.org/covid-vaccinations?country=USA)). However, vaccine-induced immunity wanes over time,  
440 making vaccines less effective against SARS-CoV-2 variants [5-7]. To assess the

441 longevity of CVXGA1, we compared one (1X CVXGA1) and two (2X CVXGA1)  
442 intranasal doses of CVXGA1 to two intramuscular doses of a mRNA COVID-19 vaccine  
443 (2X mRNA) in hamsters over time (Figure 6A). Blood was collected 7 and 79 days  
444 following the second immunization and anti-SARS-CoV-2-S IgG antibodies were  
445 quantified via ELISA. Hamsters who received 2X mRNA had highest anti-S ELISA titer,  
446 and 2X CVXGA1-immunized hamsters had higher anti-S titers than 1X CVXGA1-  
447 immunized hamsters, whose mean anti-WA1 S antibody titer was 50,699 on day 36 but  
448 the titers on day 108 are comparable for all three vaccines (Figure 6B). To assess the  
449 neutralizing ability of the antibodies, the hamster serum was tested in  
450 microneutralization assays with SARS-CoV-2 WA1, delta variant, and omicron variant.  
451 While 2X mRNA generated a high level of anti-WA1 neutralizing antibody (4,257 at 7  
452 days post-second dose), 2X CVXGA1 generated comparable levels of anti-S ELISA  
453 titers but higher levels of anti-WA1 neutralizing antibodies at day 108 (Figure 6B & C).  
454 Consistent with reduced cross-reactivity of mRNA-generated antibodies with delta and  
455 omicron variants, delta- and omicron-neutralizing antibody levels were lower than anti-  
456 WA1 in hamsters immunized with 2X mRNA at 531 and 286 respectively at 7 days post-  
457 second dose. As expected, 1X and 2X CVXGA1 generated anti-delta neutralization  
458 levels lower than anti-WA1 neutralization levels and even lower for anti-omicron (Figure  
459 6C).

460 To compare longevity of antibody responses in the hamsters, sera were collected  
461 79 days after boost (day 108 after initial immunization). Anti-S ELISA titers dropped  
462 during this time to 41.9%, 44.2%, and 73.3% for 2X mRNA, 2X CVXGA1, and 1X

463 CVXGA1, respectively (Figure 6B). Reduction of neutralizing antibody titers in 2X  
464 mRNA-immunized hamsters was substantial with 20, 60, and 40 percent of hamsters  
465 having no detectable WA1-, delta-, and omicron-neutralizing antibodies at 79 days post-  
466 boost. In contrast, serum from all hamsters immunized with 2X CVXGA1 maintained  
467 levels of neutralizing antibodies against WA1, delta variant, and omicron variant better  
468 than the 2X mRNA vaccine group (Figure 6C).

469         Eighty-seven days after the second immunization, the hamsters were challenged  
470 with delta variant and the hamster weights were monitored for 5 days. Compared to  
471 hamsters who were immunized with PBS, hamsters who received two doses of  
472 CVXGA1 had significant weight gain following challenge. Hamsters who received two  
473 doses of mRNA vaccine did experience weight gain but it was not statistically significant  
474 from the PBS group (Figure 6D). Viral burden in the hamster lungs at 5 dpc was tested  
475 by plaque assay and RT-qPCR. While PBS-immunized hamsters had mean lung titers  
476 of  $5.2 \times 10^3$  FFU/mL lung homogenate, none of the vaccinated hamsters had detectable  
477 infectious virus in their lung homogenate (Figure 6E). However, all hamsters immunized  
478 with two doses of mRNA vaccine had SARS-CoV-2 vRNA levels indicative of infectious  
479 virus with the mean CT value equating to 38 PFU per RT-qPCR reaction (Figure 6F).

480

481 **Boosting with CVXGA improves protection of hamsters immunized with mRNA**

482 **COVID-19 vaccine**

483         Due to large populations having already been immunized with COVID-19  
484 vaccines, we investigated the use of CVXGA vaccines as a booster in the hamster

485 model (Figure 6A, group 2). We used 2X mRNA immunization as a starting point for  
486 comparison. Hamsters were first immunized with two doses of mRNA COVID-19  
487 vaccine. At 62 days after second dose of mRNA vaccination, hamsters were boosted  
488 with mRNA (total 3X mRNA vaccine doses), CVXGA1, CVXGA3, CVXGA14, or PBS.  
489 Seventeen days after the third immunization, blood was collected from the hamsters  
490 and anti-WA1 S IgG antibodies were quantified via ELISA. Hamsters who received  
491 intranasal boosts of CVXGA1 (group 2B), CVXGA13 (group 2C), or CVXGA14 (group  
492 2E) had anti-S IgG titers greater than  $5 \log_{10}$ , while hamsters who received a mRNA  
493 vaccine boost (group 2A) or no boost (group 2D) had lower anti-S IgG titers (Figure 7A).  
494 In neutralization assays with WA1, delta variant, and omicron variant, there was  
495 negligible difference in average neutralization titer between sera from hamsters who  
496 received a mRNA boost to hamsters who received no boost. However, boosting with  
497 mRNA increased detectable levels of neutralizing anti-WA1, delta and omicron from 4, 2  
498 and 3 of 5 animals to 5, 3 and 5 of 5 respectively, indicating that a mRNA boost  
499 modestly increased neutralizing antibody responses (Figure 7B). In contrast,  
500 significantly higher levels of neutralizing antibodies against WA1, delta variant, and  
501 omicron variant were observed in hamsters boosted with CVXGA1, CVXGA13, or  
502 CVXGA14 (Figure 7B).

503         Twenty-five days following the boost, the hamsters were challenged with delta  
504 variant. Hamsters who received intranasal boosts of CVXGA14 or CVXGA1 had the  
505 best weight gain compared to hamsters received PBS, no boost, or an mRNA boost.  
506 Interestingly, hamsters who received CVXGA14 experienced higher weight gain than

507 hamsters who received CVXGA13 (homologous delta S antigen) (Figure 7C). None of  
508 the boosted hamsters had detectable infectious virus in their lung homogenate at 5 dpc  
509 (Figure 7D; LOD, 25 PFU/mL). However, high levels of viral RNA were detected in  
510 animals with only two doses of mRNA. CVXGA-boosted animals had the least amount  
511 of viral RNA while mRNA-boosted animals had higher levels of viral RNA among all  
512 boosted groups (Figure 7E).

513

514

515  
516

## Discussion

517           A PIV5-vectored SARS-CoV-2 vaccine expressing S (CVXGA1) has been shown  
518 to be efficacious against SARS-CoV-2 WA1 strain in mice and ferrets [17] and is  
519 currently in human clinical trials in the US. In this work, we demonstrated that one  
520 intranasal immunization of CVXGA1 protects hamsters against homologous WA1 and  
521 heterologous alpha and delta virus challenge (Figure 4, 5 and 6). Compared to 2X  
522 mRNA vaccine immunization, 2X CVXGA1 and 1X CVXGA1 generated lower anti-S  
523 binding antibody (Figure 6B), yet, anti-WA1 neutralizing antibody titers were similar  
524 among these immunization groups (Figure 6C). It is possible that because the S protein  
525 expressed by CVXGA1 is functional as indicated by their ability to promote syncytial  
526 (Figure 2), likely of native conformation (which may contain both pre- and post-fusion  
527 form of the S protein), CVXGA1 immunization may generate more cross-reactive and  
528 functional antibody responses than a mRNA vaccine. Seventy-two days post-boost  
529 immunization (at 108 dpi), anti-S antibody ELISA titers were similar among all the  
530 immunization regimens (Figure 6B). However, WA1-neutralizing antibody levels were  
531 highest in the 2X CVXGA1 group and lowest in the 2X mRNA group, indicating that  
532 CVXGA1 immunization maintains neutralizing antibody levels better than 2X mRNA  
533 immunization. The rapid reduction of neutralizing antibody titers in hamster following 2X  
534 mRNA vaccine immunization (Figure 3C) is consistent with reports of rapid reduction of  
535 neutralizing antibody titers after two doses of mRNA vaccine immunization [30]. The  
536 long-lasting neutralizing antibody levels from CVXGA1 immunization (Figure 6B and  
537 Figure 6C) may be attributed to the intranasally-expressed S antigen delivered by the

538 live replicating PIV5 vector. While a single dose intranasal immunization with CVXGA1  
539 protects hamsters against WA1 or VOCs alpha and delta, 2X CVXGA1 generates  
540 longer-lasting immunity (Figure 6C), better body weight gain after challenge (Figure 6D),  
541 and lower viral load as judged by viral RNA levels after challenge (Figure 6F), indicating  
542 that boosting CVXGA1-immunized animal with CVXGA1 affords additional protection.

543 Most of the US population has received at least one COVID-19 immunization  
544 (<https://covid.cdc.gov/covid-data-tracker>). Fully vaccinated individuals have omicron-  
545 neutralizing antibody titers 22-fold lower than WA1-neutralizing antibody titers [31] and  
546 individuals having received three doses of COVID-19 mRNA vaccines BNT162b2 or  
547 mRNA-1273 have omicron-neutralizing antibody titers of 10.7- and 7.2-fold lower,  
548 respectively [32]. It has been reported that heterologous prime-boost generates more  
549 robust immune responses than homologous prime-boost [33, 34]. Therefore, we  
550 determined the immunogenicity and efficacy of CVXGA1 as a booster in hamsters  
551 immunized with 2X mRNA vaccine (Figure 7A and 7B). As expected, boosting 2X  
552 mRNA-immunized hamsters with a third dose of mRNA vaccine did not significantly  
553 increase anti-S binding antibody titers (Figure 7A) and only moderately increased  
554 neutralizing antibody titers (Figure 7B). In contrast, boosting 2X mRNA-immunized  
555 hamsters with an intranasal dose of CVXGA1 resulted in an approximate 4.6-fold  
556 increase of anti-S antibody levels (Figure 7A) and a significant increase of neutralizing  
557 antibody titers (>15.7-, >13.1-, and >12.3-fold for WA1, delta, and omicron, respectively)  
558 (Figure 7B). Comparing mRNA vaccine-boosted hamsters (three doses of mRNA  
559 vaccine), hamsters boosted with CVXGA1 (2X mRNA plus one dose of CVXGA1) had

560 more body weight gain (Figure 7C) and lower viral load as judged by RT-qPCR of the  
561 lungs of challenged animals (Figure 7E), indicating that boosting with CVXGA1 resulted  
562 in better outcome for hamsters than boosting with a mRNA vaccine. These results are  
563 consistent with human studies for heterologous vaccine prime-boost [33, 34].

564 While we confirmed the benefits of a heterologous prime-boost with different  
565 vaccine platforms, we also observed the advantages of a heterologous antigen prime-  
566 boost. Intriguingly, we found that boosting 2X mRNA-immunized hamsters with a viral  
567 vector expressing delta (CVXGA13) or omicron S (CVXGA14) substantially increased  
568 neutralizing antibody levels against all three strains WA1, delta variant, and omicron  
569 variant. Furthermore, boosting 2X mRNA vaccinated animals with CVXGA13 or  
570 CVXGA14 increased WA1-neutralizing antibody titers significantly better than a  
571 homologous mRNA vaccine boost (Figure 7B). The differences in antigen presentation  
572 and vaccine delivery route (intranasal for CVXGA vaccines vs. intramuscular injection  
573 for mRNA vaccines) may have contributed to the more robust antibody responses  
574 induced by a CVXGA vaccine booster.

575 While we did not detect a clear advantage of using PIV5-vectored variant S  
576 vaccines over the ancestral S-based vaccine in alpha and delta VOC challenge in  
577 hamsters, the PIV5 vector has the capability for “plug and play” to quickly replace the  
578 target antigen. Due to the lack of pathogenicity in the hamster model, omicron was not  
579 used in our studies as a challenge virus [22]. VOC delta, to whom WA1-based mRNA  
580 vaccine has lower cross-reactive neutralizing antibodies against and causes the most  
581 body weight loss in hamsters, was chosen as the main challenge virus in our studies. It

582 will be interesting to test CVXGA14, or additional PIV5-vectored vaccine constructs,  
583 against yet-to-emerge SARS-CoV-2 variants in the future. Finally, SARS-CoV-2 N-  
584 specific immune responses may be protective. CVXGA2, expressing both S and N  
585 antigens of SARS-CoV-2 WA1, did have the most body weight gain and lowest viral  
586 load after heterologous virus challenge (Figure 4B and 4F). Thus, it appears that the N  
587 protein might offer additional protection, and its mechanism of protection will be further  
588 evaluated.

589         Due to the experimental limitation, we did not measure mucosal immunity or  
590 cellular immunity in these studies. Intranasal immunization with a live viral vector is  
591 expected to result in mucosal and cellular immunity in addition to humoral immune  
592 responses [12]. In this study, we did not detect a direct correlation between neutralizing  
593 antibody titers against delta and delta viral load, suggesting that other immune  
594 responses, such as cellular immune responses and/or mucosal immunity, might have  
595 played critical roles in protection.

596         In summary, CVXGA1, an intranasal vaccine currently being evaluated in human  
597 clinical trial in the US [23], protects against challenge with the homologous SARS-CoV-  
598 2 virus strain and heterologous VOCs as a single-dose in naïve and in mRNA-  
599 immunized hamsters. Our data suggests that CVXGA1, and other CVXGA vaccines,  
600 can serve as an effective heterologous booster to offer longer-lasting immunity to those  
601 who have received COVID-19 mRNA vaccines.

602

603

## Acknowledgements

604           We thank members of Drs. Biao He's, Mark Tompkins's, Jeff Hogan's, and Eric  
605 Lafontaine's labs for their technical support and helpful discussions. The work by Dr.  
606 Michael Gale, Jr. was supported by NIH grant AI151698 (MG). We thank the UGA  
607 Animal Resources staff.  
608  
609

610

## References

- 611 1. Zhu, N., et al., *A Novel Coronavirus from Patients with Pneumonia in China, 2019*. N Engl  
612 J Med, 2020. **382**(8): p. 727-733.
- 613 2. Wölfel, R., et al., *Virological assessment of hospitalized patients with COVID-2019*.  
614 Nature, 2020. **581**(7809): p. 465-469.
- 615 3. Huang, C., et al., *Clinical features of patients infected with 2019 novel coronavirus in  
616 Wuhan, China*. Lancet, 2020. **395**(10223): p. 497-506.
- 617 4. Ura, T., et al., *New vaccine production platforms used in developing SARS-CoV-2 vaccine  
618 candidates*. Vaccine, 2021. **39**(2): p. 197-201.
- 619 5. Planas, D., et al., *Reduced sensitivity of SARS-CoV-2 variant Delta to antibody  
620 neutralization*. Nature, 2021. **596**(7871): p. 276-280.
- 621 6. Zhang, L., et al., *The significant immune escape of pseudotyped SARS-CoV-2 variant  
622 Omicron*. Emerg Microbes Infect, 2022. **11**(1): p. 1-5.
- 623 7. Feikin, D.R., et al., *Duration of effectiveness of vaccines against SARS-CoV-2 infection  
624 and COVID-19 disease: results of a systematic review and meta-regression*. Lancet, 2022.  
625 **399**(10328): p. 924-944.
- 626 8. Hull, R.N., J.R. Minner, and J.W. Smith, *New viral agents recovered from tissue cultures  
627 of monkey kidney cells. I. Origin and properties of cytopathogenic agents S.V.1, S.V.2,  
628 S.V.4, S.V.5, S.V.6, S.V.11, S.V.12 and S.V.15*. Am J Hyg, 1956. **63**(2): p. 204-15.
- 629 9. Paterson, R.G., T.J. Harris, and R.A. Lamb, *Analysis and gene assignment of mRNAs of a  
630 paramyxovirus, simian virus 5*. Virology, 1984. **138**(2): p. 310-23.
- 631 10. Li, Z., et al., *Recombinant parainfluenza virus 5 expressing hemagglutinin of influenza A  
632 virus H5N1 protected mice against lethal highly pathogenic avian influenza virus H5N1  
633 challenge*. J Virol, 2013. **87**(1): p. 354-62.
- 634 11. Chen, Z., et al., *A novel rabies vaccine based on a recombinant parainfluenza virus 5  
635 expressing rabies virus glycoprotein*. J Virol, 2013. **87**(6): p. 2986-93.
- 636 12. Wang, D., et al., *A Single-Dose Recombinant Parainfluenza Virus 5-Vectored Vaccine  
637 Expressing Respiratory Syncytial Virus (RSV) F or G Protein Protected Cotton Rats and  
638 African Green Monkeys from RSV Challenge*. J Virol, 2017. **91**(11).
- 639 13. Chen, Z., et al., *Efficacy of parainfluenza virus 5 (PIV5)-based tuberculosis vaccines in  
640 mice*. Vaccine, 2015. **33**(51): p. 7217-7224.
- 641 14. Lafontaine, E.R., et al., *The autotransporter protein BatA is a protective antigen against  
642 lethal aerosol infection with Burkholderia mallei and Burkholderia pseudomallei*. Vaccine  
643 X. 2018 Dec 22;1:100002. doi: 10.1016/j.jvacx.2018.100002. eCollection 2019 Apr 11.
- 644 15. Li, K., et al., *Single-Dose, Intranasal Immunization with Recombinant Parainfluenza Virus  
645 5 Expressing Middle East Respiratory Syndrome Coronavirus (MERS-CoV) Spike Protein  
646 Protects Mice from Fatal MERS-CoV Infection*. mBio, 2020. **11**(2).
- 647 16. Xiao, P., et al., *Parainfluenza Virus 5 Priming Followed by SIV/HIV Virus-Like-Particle  
648 Boosting Induces Potent and Durable Immune Responses in Nonhuman Primates*. Front  
649 Immunol, 2021. **12**: p. 623996.
- 650 17. An, D., et al., *Protection of K18-hACE2 mice and ferrets against SARS-CoV-2 challenge by  
651 a single-dose mucosal immunization with a parainfluenza virus 5-based COVID-19  
652 vaccine*. Sci Adv, 2021. **7**(27).

- 653 18. Chan, J.F., et al., *Simulation of the Clinical and Pathological Manifestations of*  
654 *Coronavirus Disease 2019 (COVID-19) in a Golden Syrian Hamster Model: Implications*  
655 *for Disease Pathogenesis and Transmissibility*. Clin Infect Dis, 2020. **71**(9): p. 2428-2446.
- 656 19. Mohandas, S., et al., *SARS-CoV-2 Delta Variant Pathogenesis and Host Response in*  
657 *Syrian Hamsters*. Viruses, 2021. **13**(9).
- 658 20. van Doremalen, N., et al., *Efficacy of ChAdOx1 vaccines against SARS-CoV-2 Variants of*  
659 *Concern Beta, Delta and Omicron in the Syrian hamster model*. Res Sq, 2022.
- 660 21. Cochin, M., et al., *The SARS-CoV-2 Alpha variant exhibits comparable fitness to the*  
661 *D614G strain in a Syrian hamster model*. Commun Biol, 2022. **5**(1): p. 225.
- 662 22. McMahan, K., et al., *Reduced pathogenicity of the SARS-CoV-2 omicron variant in*  
663 *hamsters*. Med (N Y), 2022. **3**(4): p. 262-268.e4.
- 664 23. ClinicalTrials.gov. *Phase 1 Study of Intranasal PIV5-vectored COVID-19 Vaccine*  
665 *Expressing SARS-CoV-2 Spike Protein in Healthy Adults (CVXGA1-001)*. 2021.
- 666 24. He, B., et al., *Recovery of infectious SV5 from cloned DNA and expression of a foreign*  
667 *gene*. Virology, 1997. **237**(2): p. 249-60.
- 668 25. Lieberman, J.A., et al., *Comparison of Commercially Available and Laboratory-Developed*  
669 *Assays for In Vitro Detection of SARS-CoV-2 in Clinical Laboratories*. J Clin Microbiol,  
670 2020. **58**(8).
- 671 26. Addetia, A., et al., *Sensitive Recovery of Complete SARS-CoV-2 Genomes from Clinical*  
672 *Samples by Use of Swift Biosciences' SARS-CoV-2 Multiplex Amplicon Sequencing Panel*. J  
673 Clin Microbiol, 2020. **59**(1).
- 674 27. O'Toole, Á., et al., *Assignment of epidemiological lineages in an emerging pandemic*  
675 *using the pangolin tool*. Virus Evol, 2021. **7**(2): p. veab064.
- 676 28. Blanchard, E.L., et al., *Treatment of influenza and SARS-CoV-2 infections via mRNA-*  
677 *encoded Cas13a in rodents*. Nat Biotechnol, 2021. **39**(6): p. 717-726.
- 678 29. Tompkins, S.M., et al., *Recombinant parainfluenza virus 5 (PIV5) expressing the influenza*  
679 *A virus hemagglutinin provides immunity in mice to influenza A virus challenge*. Virology,  
680 2007. **362**(1): p. 139-50.
- 681 30. Fang, Z., et al., *Omicron-specific mRNA vaccination alone and as a heterologous booster*  
682 *against SARS-CoV-2*. bioRxiv, 2022.
- 683 31. Cele, S., et al., *SARS-CoV-2 Omicron has extensive but incomplete escape of Pfizer*  
684 *BNT162b2 elicited neutralization and requires ACE2 for infection*. medRxiv, 2021.
- 685 32. Regev-Yochay, G., et al., *Efficacy of a Fourth Dose of Covid-19 mRNA Vaccine against*  
686 *Omicron*. N Engl J Med, 2022. **386**(14): p. 1377-1380.
- 687 33. Atmar, R.L., et al., *Homologous and Heterologous Covid-19 Booster Vaccinations*. N Engl  
688 J Med, 2022. **386**(11): p. 1046-1057.
- 689 34. Costa Clemens, S.A., et al., *Heterologous versus homologous COVID-19 booster*  
690 *vaccination in previous recipients of two doses of CoronaVac COVID-19 vaccine in Brazil*  
691 *(RHH-001): a phase 4, non-inferiority, single blind, randomised study*. Lancet, 2022.  
692 **399**(10324): p. 521-529.
- 693

695  
696

## Figure legends

697

### 698 **Figure 1. Schematics of PIV5 and CVXGA vaccines.**

699 The PIV5 genome has 7 genes 3' to 5': NP, V/P, M, F, SH, HN, L. The S genes from  
700 SARS-CoV-2 WA1 (CVXGA1), beta variant (CVXGA3), gamma variant (CVXGA5),  
701 delta variant (CVXGA13), and omicron variant (CVXGA14) had their cytoplasmic tails  
702 replaced with the PIV5 F cytoplasmic tail and inserted between PIV5 SH and HN genes.  
703 CVXGA2 also has SARS-CoV-2 WA1 N inserted between PIV5 HN and L genes.

704

### 705 **Figure 2. CVXGA vaccine antigen expression.**

706 Vero cells were infected at MOI 0.01 for 3 days. (A) Cell-to-cell fusion induced by  
707 SARS-CoV-2 S expression was imaged at 10X with an Evos M5000 microscope.  
708 Arrows indicate syncytium, multinucleated cells. (B) Intracellular expression of PIV5-  
709 V/P, SARS-CoV-2-S, and SARS-CoV-2-N was detected by anti-PIV5 V/P, -SARS-CoV-  
710 2 S, or SARS-CoV-2 N antibodies, followed by Cy3-conjugated secondary antibody, and  
711 imaged at 10X with an EVOS M5000 microscope (Thermo Fisher Scientific).

712

### 713 **Figure 3. Immunization of hamsters with CVXGA1, CVXGA2, CVXGA3, and** 714 **CVXGA5 induces anti-SARS-CoV-2 S IgG antibodies.**

715 (A) Schematic of hamster study AE19 immunization. Golden Syrian hamsters (n=8)  
716 were intranasally immunized with 100  $\mu$ L of  $10^5$  PFU PIV5, CVXGA1, CVXGA2,  
717 CVXGA3, or CVXGA5. Blood was collected at 28 dpi. At 36 dpi, four hamsters from

718 each group were challenged with  $10^3$  PFU of SARS-CoV-2 Wuhan strain (WA1) and the  
719 remaining four hamsters were challenged with  $10^3$  PFU SARS-CoV-2 alpha variant.  
720 Following challenge infection, the hamster weights were monitored daily before  
721 terminating the study at 5 dpc to collect lung tissues. (B) Anti-SARS-CoV-2 S IgG  
722 antibody titers were quantified by ELISA. Antibody titers were calculated as  $\log_{10}$  of the  
723 highest serum dilution at which the OD<sub>450</sub> was greater than two standard deviations  
724 above the mean OD<sub>450</sub> of naïve serum. The lower limit of detection (LOD) and upper  
725 limit of detection (ULOD) are indicated by the dotted lines. Bars represent the geometric  
726 means. Comparing each group to the vector control, statistical significance was  
727 calculated with one-way ANOVA (\*\*\*\*  $p < 0.0001$ ).

728

729 **Figure 4. Immunization with CVXGA1 protects hamsters from challenge with**  
730 **SARS-CoV-2 WA1 and alpha variant.**

731 Following challenge with WA1 (A) or alpha variant (B), hamster weights were monitored  
732 daily for five days and graphed as percent day 0 weight. Statistical significance was  
733 calculated for each timepoint between each group and PIV5-immunized hamsters with t  
734 tests (\*  $p \leq 0.05$ , \*\*  $p < 0.01$ , \*\*\*  $p < 0.001$ , \*\*\*\*  $p < 0.0001$ ). At 5 dpc with WA1 (C) or  
735 alpha variant (D), viral load in hamster lung was quantified via plaque assay in Vero E6  
736 cells and graphed as PFU/mL lung homogenate. The limit of detection (LOD) is  
737 indicated by the dotted line. Error bars represent the standard error of the means.  
738 SARS-CoV-2 WA1 (E) or alpha variant (F) vRNA load in lung homogenates was  
739 quantified via RT-qPCR. The cycle threshold (Ct) value for each sample is presented

740 and error bars represent the standard error of the means. The known viral titers of WA1  
741 and alpha variant were used to generate standard curves for E and F, respectively, and  
742 the Ct values equating to 1 PFU per reaction (rxn) were calculated. The Ct value  
743 generated from RNA extracted from sterile water is denoted by a dotted line labelled  
744 PCR negative. The limit of detection (LOD) is indicated by a dotted line at Ct value = 40,  
745 the number of PCR cycles. Comparing each group to PIV5-immunized hamsters,  
746 statistical significance was calculated with one-way ANOVA (\*\*  $p < 0.01$ , \*\*\*  $p < 0.001$ ).

747

748 **Figure 5. Immunization with CVXGA1 protects hamsters from challenge with**  
749 **SARS-CoV-2 delta variant.**

750 (A) Schematic of hamster study AE23 immunization. Golden Syrian hamsters ( $n=5$ )  
751 were intranasally immunized with 100  $\mu\text{L}$  PBS,  $3 \times 10^5$  PFU CVXGA1,  $2 \times 10^5$  PFU  
752 CVXGA3, or  $1.5 \times 10^5$  PFU CVXGA13. Blood was collected at 19 dpi. At 28 dpi, the  
753 hamsters were challenged with  $10^4$  PFU of SARS-CoV-2 delta variant. Following  
754 challenge infection, the hamster weights were monitored daily before terminating the  
755 study and harvesting lungs at 5 dpc. Anti-SARS-CoV-2 WA1 S (B) and RBD (C) IgG  
756 antibodies were quantified via ELISA at 19 dpi. Antibody titer was calculated as  $\log_{10}$  of  
757 the highest serum dilution at which the  $\text{OD}_{450}$  was greater than two standard deviations  
758 above the mean  $\text{OD}_{450}$  of naïve serum. The limit of detection (LOD) is indicated by the  
759 dotted line. Error bars represent the standard error of the means. Comparing each  
760 group to the vector control, statistical significance was calculated with one-way ANOVA  
761 (\*\*  $p < 0.01$ , \*\*\*\*  $p < 0.0001$ ). (D) Following challenge infection, hamster body weights

762 were monitored daily for five days and graphed as percent of day 0 weight. Statistical  
763 significance was calculated for each timepoint between each group and PIV5-  
764 immunized hamsters with t tests (\*  $p \leq 0.05$ , \*\*  $p < 0.01$ , \*\*\*  $p < 0.001$ ). (E) Viral load in  
765 lung homogenate was quantified via plaque assay in Vero TEMPRSS cells and graphed  
766 as PFU/mL lung homogenate. The limit of detection (LOD) is indicated by the dotted  
767 line. Error bars represent the standard error of the means. (F) RNA was extracted from  
768 lung homogenate and SARS-CoV-2 delta vRNA was quantified via RT-qPCR. The cycle  
769 threshold (Ct) value for each sample is presented and error bars represent the standard  
770 error of the means. The known viral titer of delta variant was used to generate a  
771 standard curve to calculate the Ct value equating to 1 PFU per reaction (rxn). The limit  
772 of detection (LOD), PCR negative, is indicated by a dotted line at Ct value = 40, the  
773 number of PCR cycles.

774

775 **Figure 6. Immunization with a COVID-19 mRNA vaccine, one dose of CVXGA1, or**  
776 **two doses of CVXGA1 protects hamsters against challenge with delta variant.**

777 (A) Schematic of hamster study AE24 immunization. Golden Syrian hamsters received  
778 100  $\mu$ L PBS intranasally (n=5, Group 1), 2  $\mu$ g mRNA COVID vaccine (n=25, Group 2),  
779 or 100  $\mu$ L  $7 \times 10^4$  PFU CVXGA1 (n=10, Groups 3 & 4). At 29 dpi, hamsters that received  
780 the mRNA vaccine were boosted with the mRNA vaccine and group 3 hamsters  
781 received another dose of CVXGA1. At 91 dpi following initial immunization, hamsters  
782 who received two doses of mRNA received 2  $\mu$ g mRNA vaccine (n=5, Group 2A),  $7 \times 10^4$   
783 PFU CVXGA1 (n=5, Group 2B),  $10^3$  PFU CVXGA13 (n=5, Group 2C), PBS i.n. (n=5,

784 Group 2D), or  $10^4$  PFU CVXGA14 (n=5, Group 2E). Blood was collected at 36 and 108  
785 dpi. At 116 dpi, the hamsters were challenged with  $10^5$  PFU SARS-CoV-2 delta variant.  
786 Following challenge infection, hamster weights were monitored for 5 days and the lungs  
787 were harvested. (B) Anti-SARS-CoV-2 WA1 S IgG antibodies were quantified via ELISA  
788 at 36 and 108 days post-immunization. Antibody titer was calculated as  $\log_{10}$  of the  
789 highest serum dilution at which the  $OD_{450}$  was greater than two standard deviations  
790 above the mean  $OD_{450}$  of naïve serum. The limit of detection (LOD) is indicated by the  
791 dotted line. The geometric means are presented in the table and represented as bars on  
792 the graph. (C) Microneutralizing antibody titers against SARS-CoV-2 WA1, delta, or  
793 omicron were calculated as  $\log_{10}$  of the highest serum dilution at which the virus  
794 infectivity was reduced by at least 50%. The limit of detection (LOD) is indicated by the  
795 dotted line. The geometric means are presented in the table and represented as bars on  
796 the graph. (D) Following challenge, hamster weights were monitored daily for five days  
797 and graphed as percent of day 0 weight. Statistical significance was calculated for each  
798 timepoint between each group and PBS-immunized hamsters with t tests (\*  $p \leq 0.05$ ).  
799 (E) Viral load in lung homogenate at 5 dpc was quantified via plaque assay in Vero  
800 TEMPRSS cells and graphed as PFU/mL lung homogenate. The limit of detection  
801 (LOD) is indicated by the dotted line. Error bars represent the standard error of the  
802 means. (F) Viral RNA load in lung homogenate was quantified via RT-qPCR. The cycle  
803 threshold (Ct) value for each sample is presented and error bars represent the standard  
804 error of the means. The known viral titer of delta variant was used to generate a  
805 standard curve and calculate the Ct value equating to 1 PFU per reaction (rxn). The Ct

806 value generated from RNA extracted from sterile water is denoted by a dotted line  
807 labelled PCR negative. The limit of detection (LOD) is indicated by a dotted line at Ct  
808 value = 40, the number of PCR cycles. Error bars represent the standard error of the  
809 means. Statistical significance was calculated with one-way ANOVA (\*\*  $p < 0.01$ , \*\*\*\*  $p$   
810  $< 0.0001$ ).

811

812 **Figure 7. CVXGA1 boosts the humoral immune response and protection of**  
813 **mRNA-immunized hamsters against challenge with delta variant.**

814 (A) Anti-SARS-CoV-2 S IgG antibodies at 17 days post-boost were quantified via ELISA.  
815 Antibody titer was calculated as  $\log_{10}$  of the highest serum dilution at which the  $OD_{450}$  was  
816 greater than two standard deviations above the mean  $OD_{450}$  of naïve serum. The limit of  
817 detection (LOD) is indicated by the dotted line. Bars represent geometric means.  
818 Statistical significance was calculated with one-way ANOVA (\*\*\*\*  $p < 0.0001$ ). (B)  
819 Microneutralizing antibody titers against SARS-CoV-2 WA1, delta, or omicron were  
820 calculated as  $\log_{10}$  of the highest serum dilution at which the virus infectivity was reduced  
821 by at least 50%. The limit of detection (LOD) is indicated by the dotted line. The geometric  
822 means are presented in the table and represented as bars on the graph. Statistical  
823 significance was calculated between each group and the PBS group or 2X mRNA group  
824 with one-way ANOVA (\*  $p \leq 0.05$ , \*\*  $p < 0.01$ , \*\*\*  $p < 0.001$ , \*\*\*\*  $p < 0.0001$ ). (C) Hamster  
825 body weight changes over five days post-challenge were graphed as percent of day 0  
826 weight. Statistical significance was calculated for each timepoint between each group and  
827 PBS-immunized hamsters with t tests (\*  $p \leq 0.05$ , \*\*  $p < 0.01$ ). (E) Viral load in lung

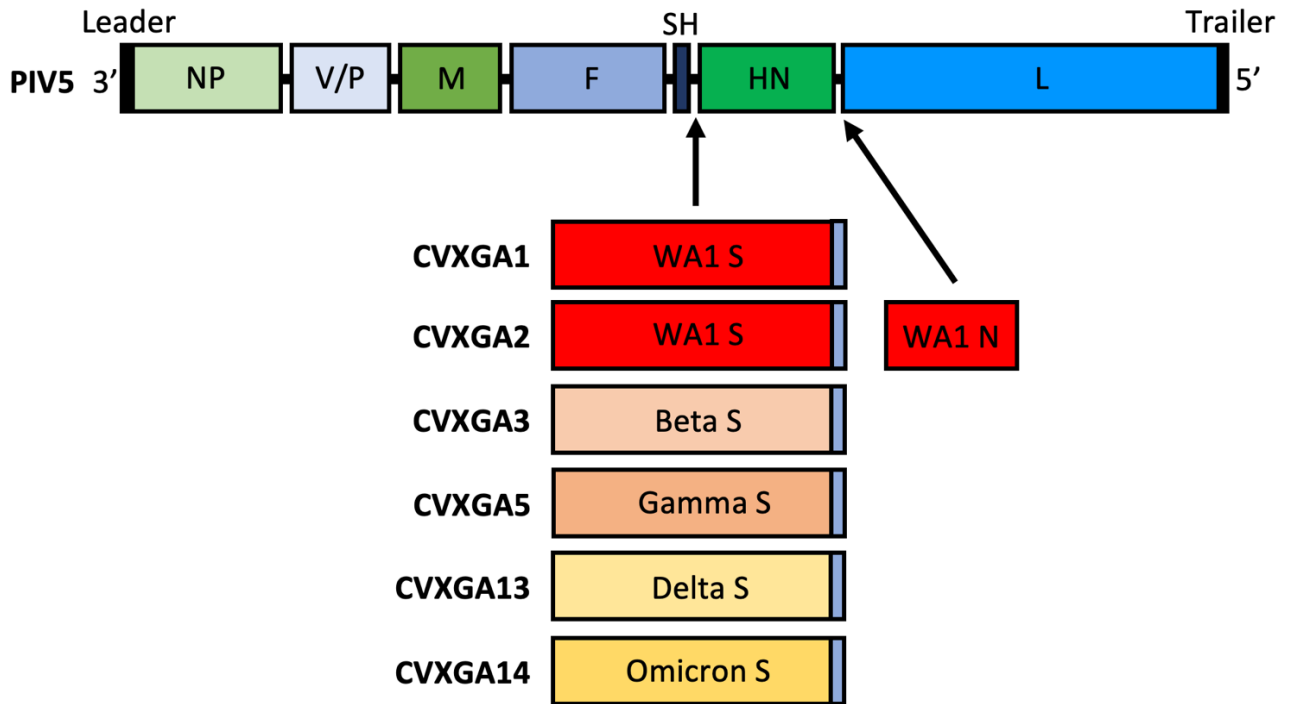
828 homogenates at 5 dpi was quantified via plaque assay in Vero TEMPRSS cells and  
829 graphed as PFU/mL lung homogenate. The limit of detection (LOD) is indicated by the  
830 dotted line. Error bars represent the standard error of the means. (F) SARS-CoV-2 delta  
831 vRNA load in lung homogenate was quantified via RT-qPCR. The cycle threshold (Ct)  
832 value for each sample is presented and error bars represent the standard error of the  
833 means. The known viral titer of delta variant was used to generate a standard curve and  
834 to calculate the Ct value equating to 1 PFU per reaction (rxn). The Ct value generated  
835 from RNA extracted from sterile water is denoted by a dotted line labelled PCR negative.  
836 The limit of detection (LOD) is indicated by a dotted line at Ct value = 40, the number of  
837 PCR cycles. Error bars represent the standard error of the means. Statistical significance  
838 was calculated with one-way ANOVA (\*\*  $p < 0.01$ , \*\*\*\*  $p < 0.0001$ ).

839

840

## Figures

841 **Figure 1**

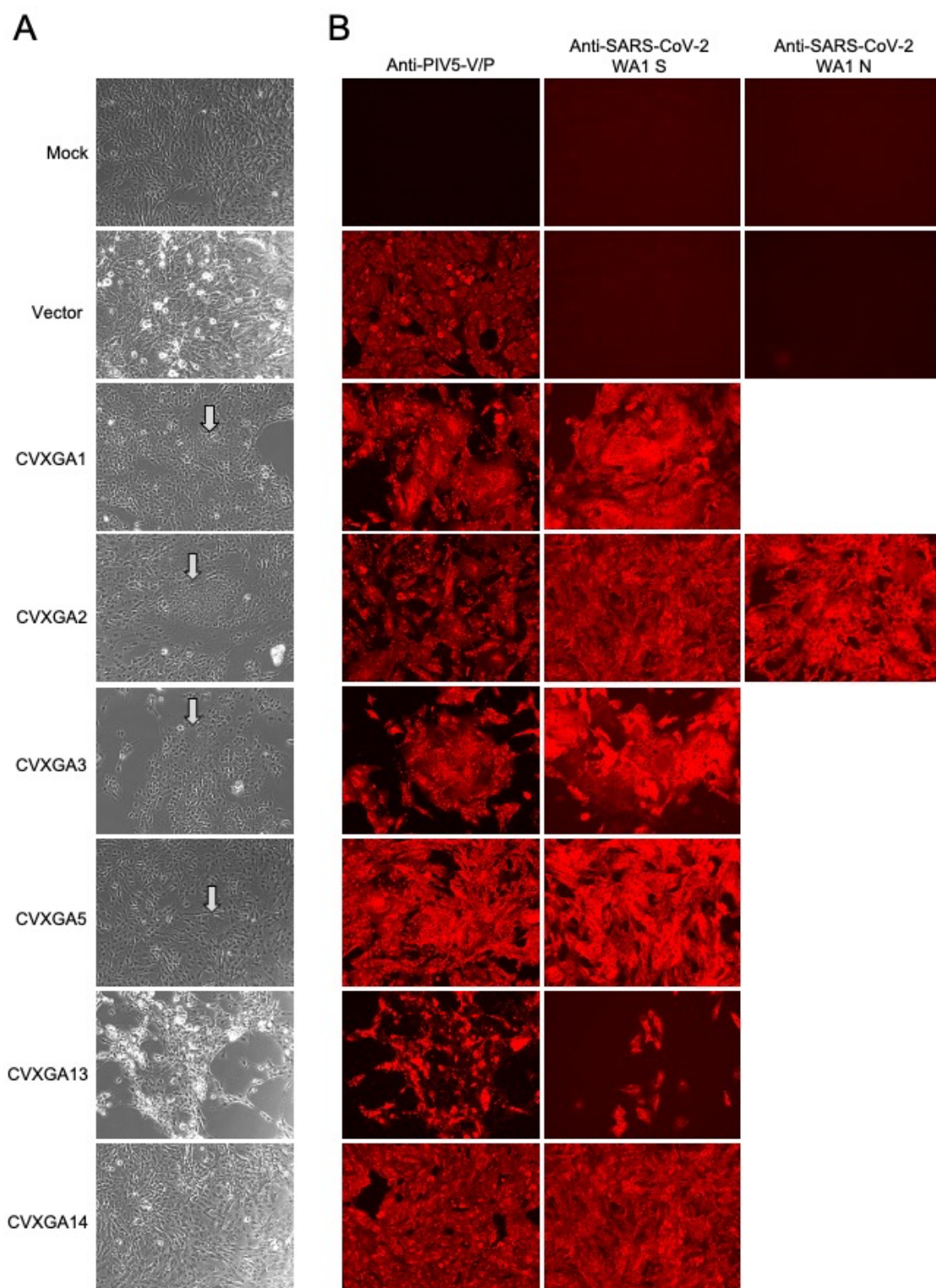


842

843

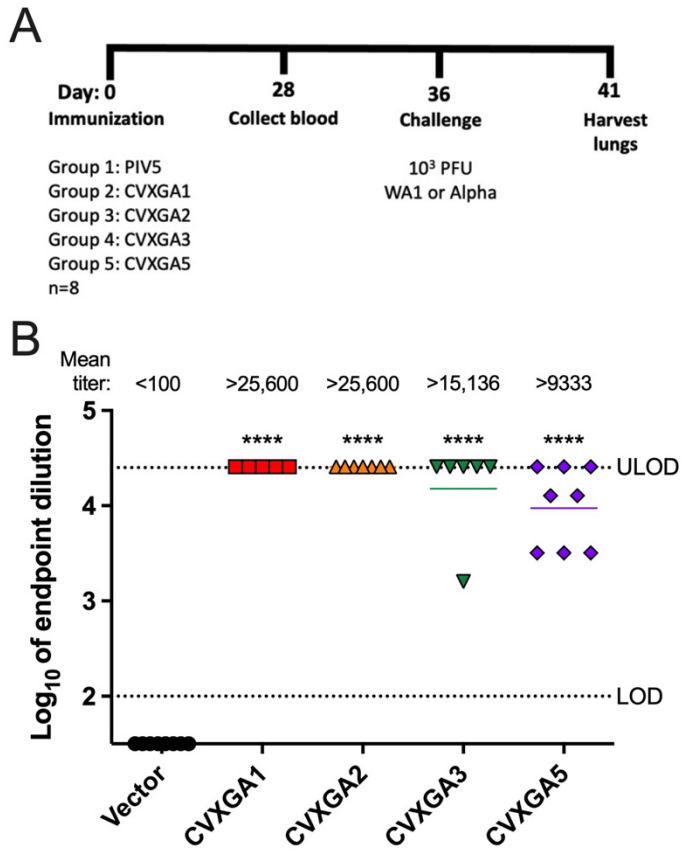
844

845 **Figure 2**



846

847 **Figure 3**

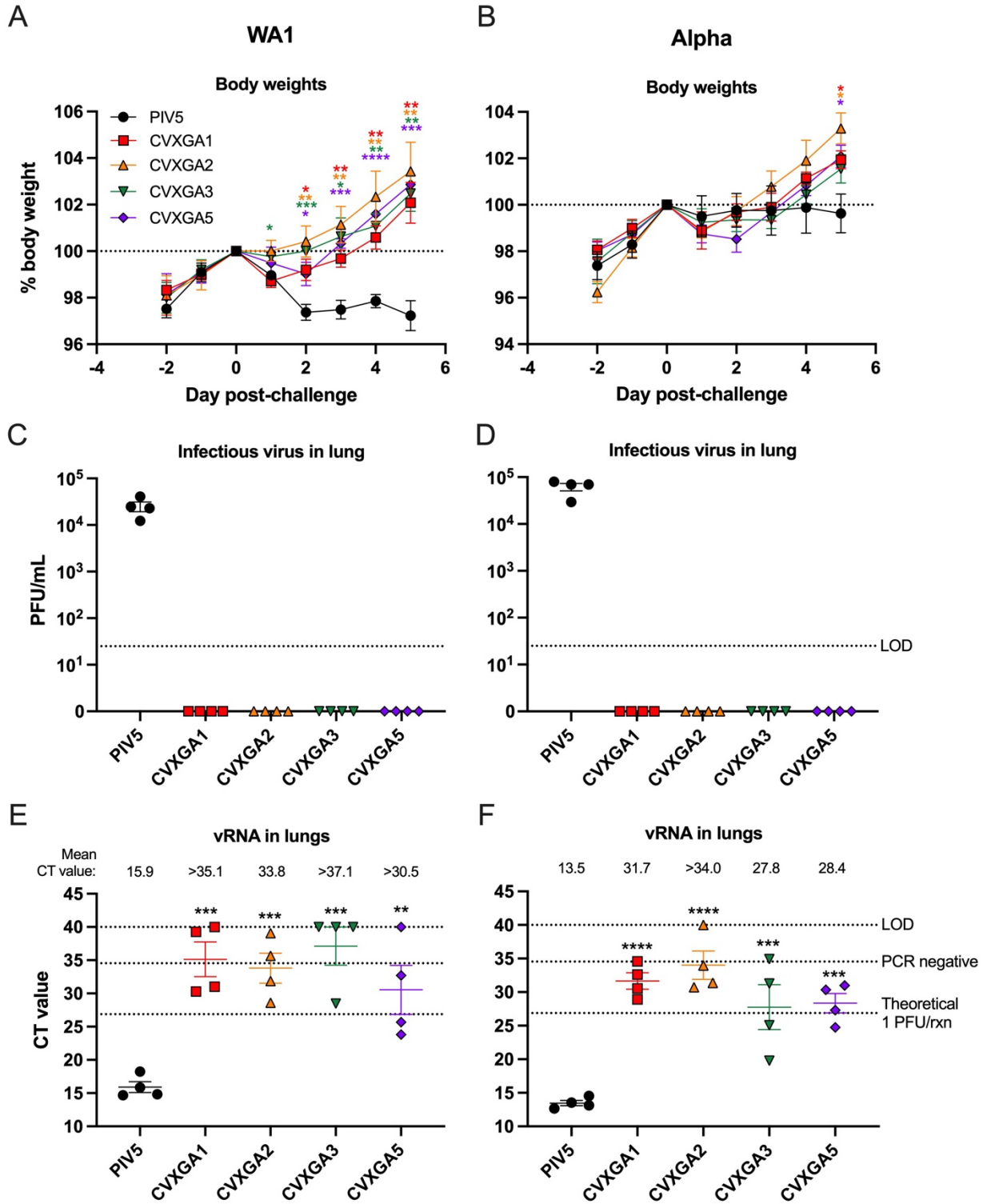


848

849

850

851 **Figure 4**



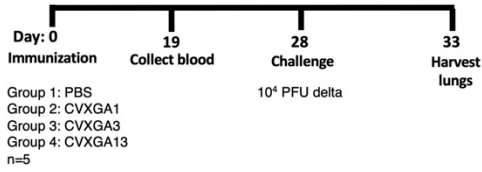
852

853

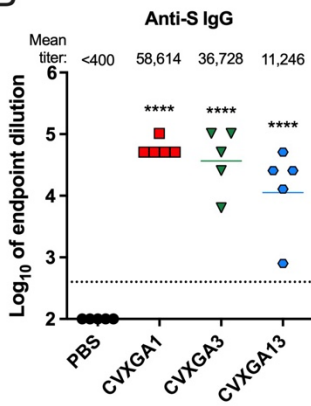
854

855 **Figure 5**

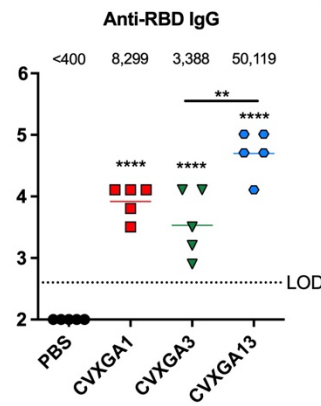
**A**



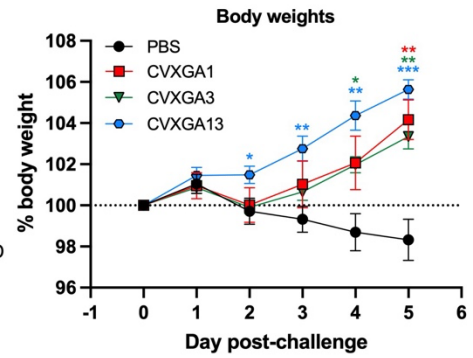
**B**



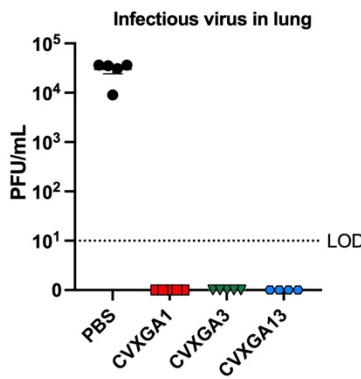
**C**



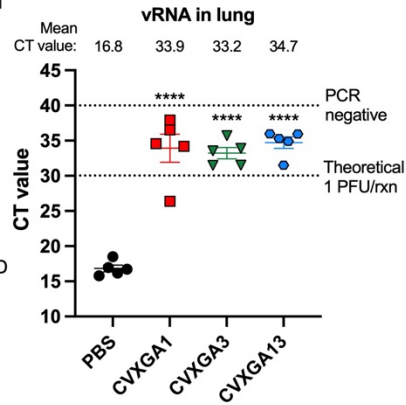
**D**



**E**



**F**

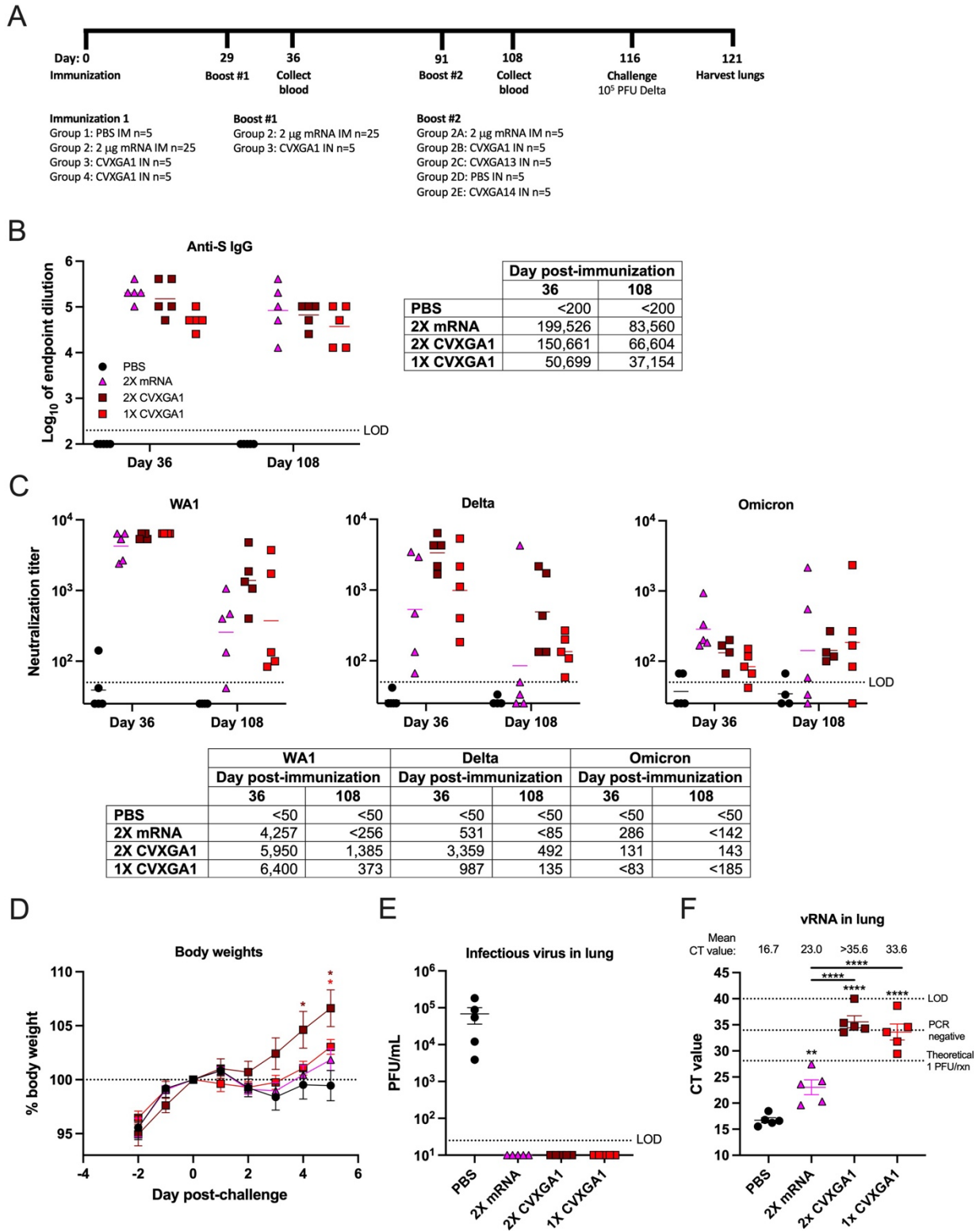


856

857

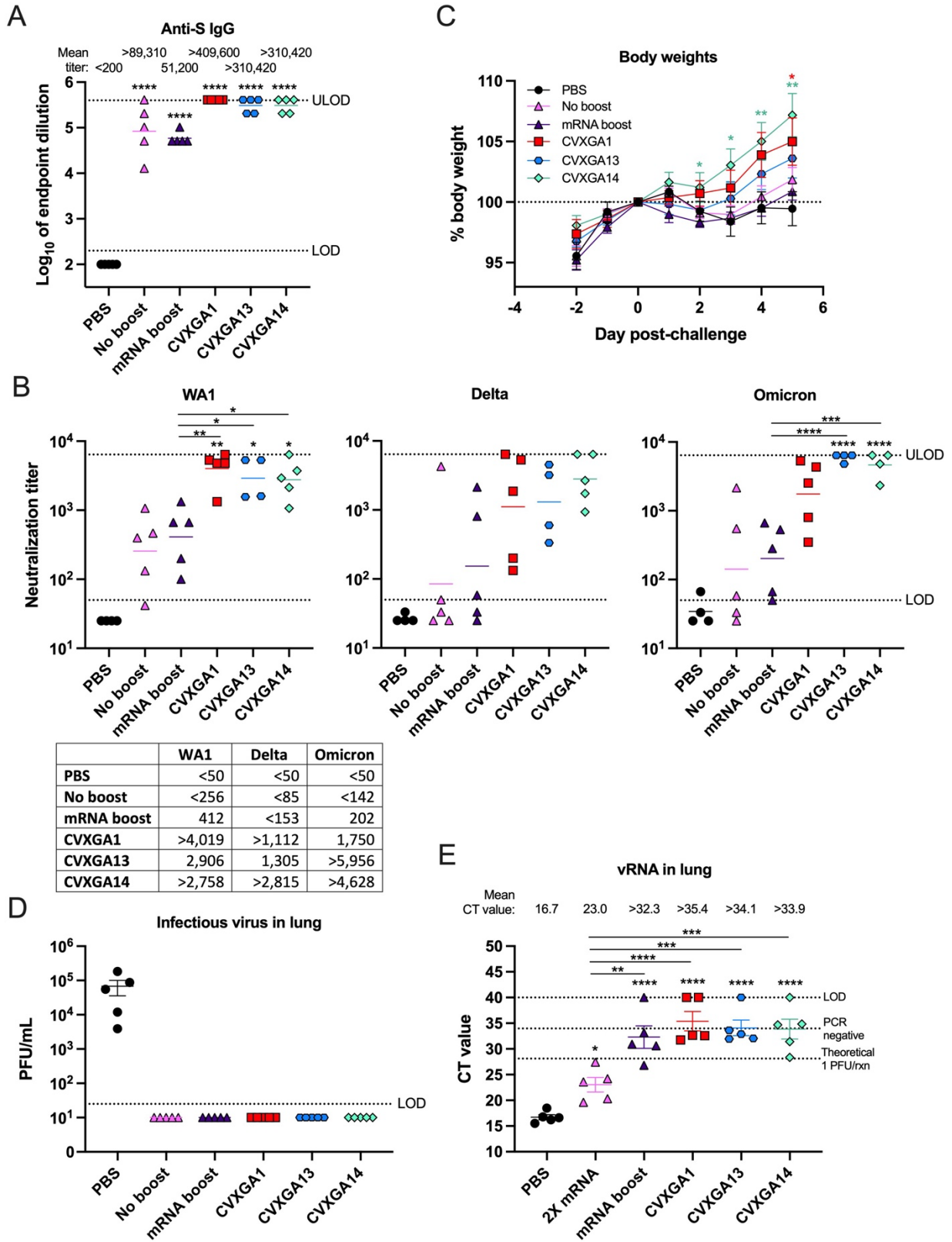
858

859 **Figure 6**



860

861 **Figure 7**



862

863

## Supplemental figure

864

865 **Supplemental figure 1. RT-qPCR standard curves.** RNA was extracted from SARS-

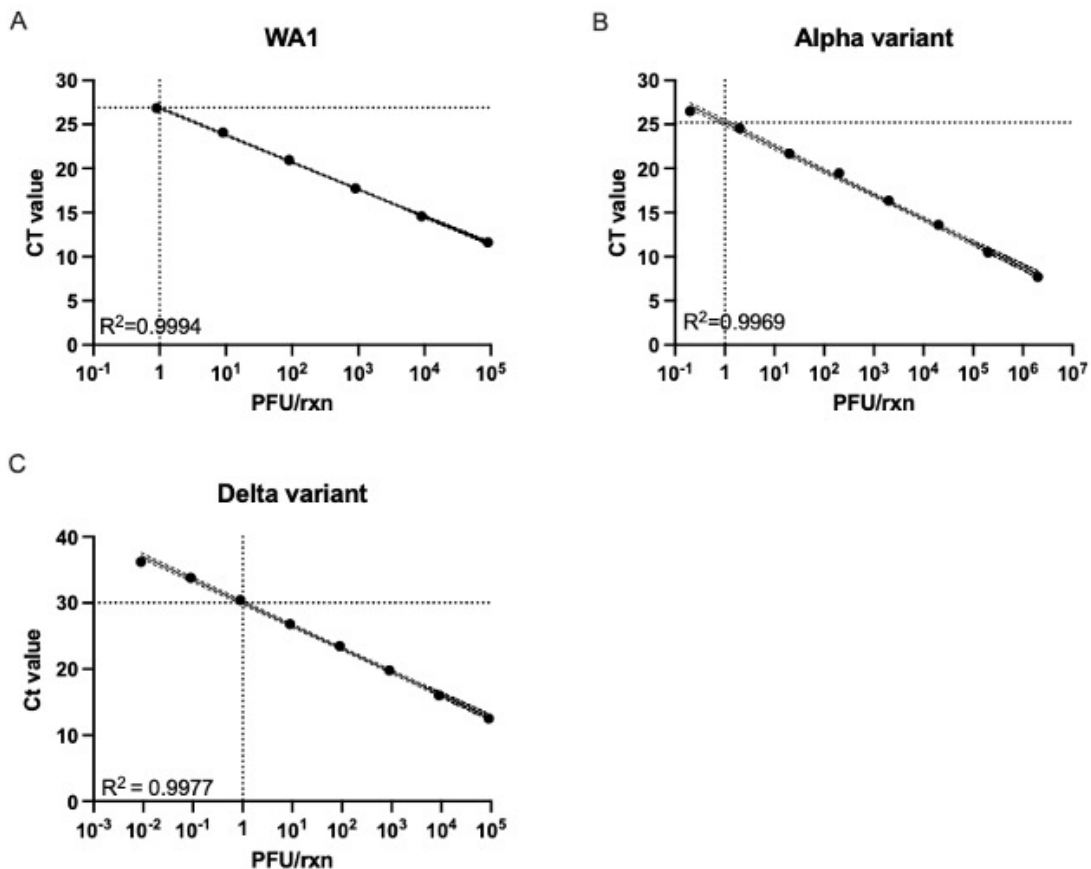
866 CoV-2 WA1 (A), alpha variant (B), and delta variant (C) viral stocks of known titer. The

867 RNA was serially diluted and vRNA was quantified via RT-qPCR. To generate a

868 standard curve, the Ct value was plotted on the y-axis and the PFU per reaction (rxn)

869 was plotted on the x-axis. Dotted lines indicate the Ct value which corresponds to 1

870 PFU/rxn.



871